Importance of the wheel vertical dynamics in the squeal noise mechanism on a scaled test bench

C. Collette
Department of Mechanical Engineering and Robotics, University of Brussels, Brussels, Belgium

Abstract. This paper investigates the influence of the wheel vertical dynamics in the mechanism of squeal noise on a scaled test bench. To this purpose, sustained oscillations are first studied on a single degree of freedom oscillator, considering both a decreasing slope of the friction curve and a vertical excitation. Their relative importance to sustain the oscillations is discussed. Then, a mathematical model of a quarter scale test bench is developed in the frequency domain. Using this model, it is shown that the squeal noise resulting from the excitation of the bending modes of the wheel is sustained because these bending modes are associated with variations of the vertical contact force. Results are further confirmed by experiments conducted on a scaled test bench.

Keywords: Squeal noise, scaled test bench, forced and self excited vibrations

1. Introduction

The first squeal noise models have been developed in the seventies [18]. The basic mechanism of squeal noise is a variation of the lateral creep force between the wheel and the rail, due to a frictional instability. The variations occur preferentially at a frequency of a lateral resonance of the wheel [12]; the instability arise from a decreasing slope of the phenomenological law linking the creepage between the wheel and the rail and the associated creep force (Fig. 1(a)). Some minimal models are presented in [23]. A more complete mathematical description of the wheel lateral dynamics has been included in [19], and later in [6,7]. An experimental validation on a scaled test bench has been presented in [4,22]. The vertical dynamics has been lately introduced in a squeal model by [1], but its role in the mechanism of squeal noise has not been investigated.

Even if quite efficient models [15,21] and solutions exist for its mitigation [14,16] (e.g. iron rings [2,3], active control [8], high positive friction [5]) the experimental validation of squeal models remains a challenging task for two reasons [17]: (i) for identical operating conditions, there exist large fluctuations in the sound levels radiated, in the mode which squeals and even in the occurrence of squeal; (ii) squeal has been recorded without any associated negative slope of the creepage-creep force law [13].

The motivation of this paper is to investigate the influence of the vertical dynamics of the wheel on the fluctuations mentioned above. Actually, as the vehicle runs over the track, the roughness of the contact surfaces creates variations of the vertical forces between the wheel and the rail. The frequencies of these variations are governed by wheel and rail vertical receptances. At low frequencies, below 1000 Hz, the rail has the highest receptance. This means

---

*Address for correspondence: Department of Mechanical Engineering and Robotics, University of Brussels, 50 av. F.D. Roosevlet, 1050 Brussels, Belgium. Tel.: +32 2 650 46 62; Fax: +32 2 650 46 60; E-mail: Christophe.Collette@ulb.ac.be.
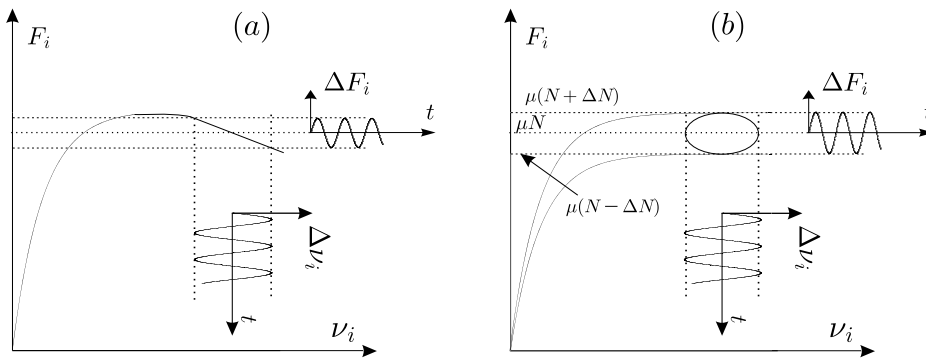
Fig. 1. Friction curves between the wheel and the rail describing two mechanisms for sustained oscillations between the wheel and the rail: (a) Decreasing slope of the friction curve after saturation; (b) Variation of the normal force.
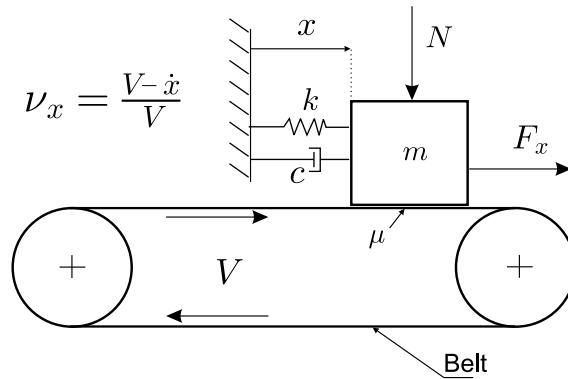

Fig. 2. Single d.o.f. oscillator excited by friction.

that the surface irregularities are mainly compensated by a displacement of the rail. The displacement creates high variations of the contact forces, responsible of rail corrugation. At higher frequencies, above 1000 Hz, the wheel has the highest receptance at its resonances, and the contact spring has the highest receptance between two wheel resonances. This means that a very short irregularity of the surface is either compensated by a displacement of the wheel, or by a local deformation of the bodies in contact. The frequency of these variations is of course much too high to corrugate the surface, because of the finite size of the contact patch. However, the variations of the vertical contact force create a variation of the creep between the wheel and the rail at the same frequency (Fig. 1(b)), which are exacerbated at frequencies corresponding to peaks in the vertical-lateral cross receptance of the wheel.

In order to precise the importance of the wheel dynamics in the mechanism of squeal generation, the phenomenon is first studied using a very simple wheel model. Then, numerical results obtained using a more complete model including the wheel dynamics are compared with experiments performed on a scaled test bench from INRETS.

2. Single d.o.f. oscillator

Figure 2 shows a single degree of freedom oscillator excited by friction over a moving belt [9]. As mentioned in the previous section, there exists two means to get sustained oscillations with an oscillator: either by a decreasing slope of the creepage-creep force phenomenological law, or by a variation of the vertical force applied to the moving mass. In the former case, the motion of the belt is transformed into *self excited vibrations* of the mass. In the latter case, the mass is subjected to a *forced vibration* imposed by the variation of the vertical force.

First consider the case of a decreasing slope. The equation of motion reads

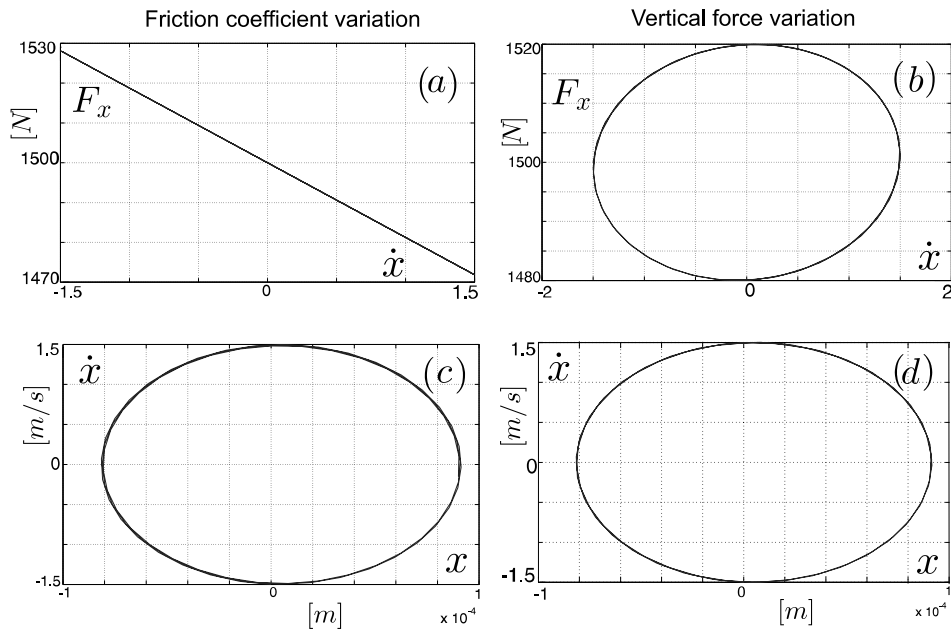$$m\ddot{x} + c\dot{x} + kx = F_x \tag{1}$$

Fig. 3. Self excited vibrations: (a) Speed – friction force and (c) Speed – displacement; forced vibrations: (b) Speed – friction force and (d) Speed – displacement.

where m is the mass of the oscillator, k the stiffness of the spring, c the damping coefficient and F_x the creep force. The dependency between the relative speed between the mass and the belt and the friction force is given by the Coulomb law:

$$F_x = (\mu - \delta\nu_x)N_0 sign(\nu_x) \tag{2}$$

where $\nu_x = (\dot{x} - V)/V$ and N_0 is the static load, and δ the decreasing slope of the friction curve. Figures 3(a) and (c) show respectively the creep force as a function of the velocity of the mass, and the velocity-displacement phase diagram. The sable limit cycle has been obtained with the following numerical values: $m = 1.1$ kg; $k = 100$ MN/m; $c = 2$ Ns/m; $\mu = 0.4$; $N_0 = 3750$ N; $\delta = 0.005$; $V = 5$ m/s.

Then, consider that the oscillator is excited harmonically by a vertical force $N = N_0 + A sin(\omega t)$. The friction force becomes

$$F_x = \mu[N_0 + A sin(\omega t)]sign(\nu_x) \tag{3}$$

where N_0 is the static load, A the amplitude of dynamic variation, $\omega = \sqrt{k/m}$

Again, Figs 3(b) and (d) show respectively the creep force as a function of the velocity of the mass, and the velocity-displacement phase diagram. The sable limit cycle has been obtained with the following numerical values: $m = 1.1$ kg; $k = 100$ MN/m; $c = 2$ Ns/m; $N_0 = 3750$ N; $A = 50$ N.

From Figs 3(c) and (d), one sees that the limit cycles obtained from the two models are exactly the same. This explains why sometimes, squeal is recorded without any measurable decreasing slope of the friction law.

Actually, the combination of these two mechanisms, discussed in [9,20] on single d.o.f. oscillators, is probably the most credible scenario of squeal noise in many cases.

3. Railway dynamics

3.1. Vertical dynamics

The vertical dynamics of the wheel-rail contact is governed by Hertz's theory, giving a non-linear relationship between the load and the deformation of the bodies in contact. This relationship can be linearized as

$$\Delta N = k_c \Delta d \tag{4}$$

where Δd is the variation of the distance between the wheel and the rail induced by a variation of the vertical force ΔN, and k_c is called the contact stiffness (typically $k_c = 1.2$ GN/m). Taking the vehicle and track dynamics into account, an irregularity of the rail surface Δz leads to a combination of a wheel displacement Δu_z^w, a rail displacement Δu_z^r, and a deformation at the wheel-rail interface Δd:

$$\Delta z = \Delta d + \Delta u_z \tag{5}$$

where $\Delta u_z = \Delta u_z^w - \Delta u_z^r$. The vertical displacements of the wheel and the rail are given by

$$\Delta u_z^w = R_{zy}^w \Delta F_y + R_{zz}^w \Delta N \tag{6}$$

$$\Delta u_z^r = -R_{zy}^r \Delta F_y - R_{zz}^r \Delta N \tag{7}$$

where R_{zz}^w and R_{zz}^r are respectively the vertical direct receptances of the vehicle and the track. The sum of these last two equations can be written as

$$\Delta u_z = +R_{zy} \Delta F_y + R_{zz} \Delta N \tag{8}$$

where $R_{ij} = R_{ij}^w + R_{ij}^r$ $(i, j = y, z)$.

3.2. Lateral dynamics

The lateral creepage ν_y between the wheel and the rail is given by

$$\nu_y = \frac{\dot{u}_y^w - \dot{u}_y^r}{V} \tag{9}$$

where u_y^w and u_y^r are respectively the lateral displacements of the wheel and the rail, and V the vehicle speed. In the frequency domain, small linear variations of the lateral creepage are expressed by

$$\Delta \nu_y = \frac{i\omega \Delta u_y}{V} \tag{10}$$

where $\Delta u_y = \Delta u_y^w - \Delta u_y^r$ and $\omega = 2\pi f = 2\pi V/l$ (f is the frequency and l the wavelength of the irregularity).

The relationship between the lateral creepage and the associated creep force between the wheel and the rail is given by a non-linear phenomenological law (e.g. [11])

$$F_y = \mu N \left[1 - \exp \frac{-C_0 \nu_y}{\mu N^{1/3}} \right] \tag{11}$$

where C_0 is a constant, $C_0 N^{2/3}$ the slope of the friction curve for $\nu_y \to 0$ and $\mu = \mu_0 - \delta \nu_y$. Again, this law can be linearized as follows

$$\Delta F_y = \frac{\partial F_y}{\partial N} \Delta N + \frac{\partial F_y}{\partial \nu_y} \Delta \nu_y \tag{12}$$

The lateral displacements of the vehicle and the track are expressed as

$$\Delta u_y^w = R_{yy}^w \Delta F_y + R_{yz}^w \Delta N \tag{13}$$

$$\Delta u_y^r = -R_{yy}^r \Delta F_y - R_{yz}^w \Delta N \tag{14}$$

where R_{yy}^w and R_{yy}^r are respectively the lateral direct receptances of the vehicle and the track; R_{yz}^w and R_{yz}^r are respectively the cross receptances of the vehicle and the track between the vertical and the lateral directions. The sum of these last two equations can be written as

$$\Delta u_y = R_{yy} \Delta F_y + R_{yz} \Delta N \tag{15}$$

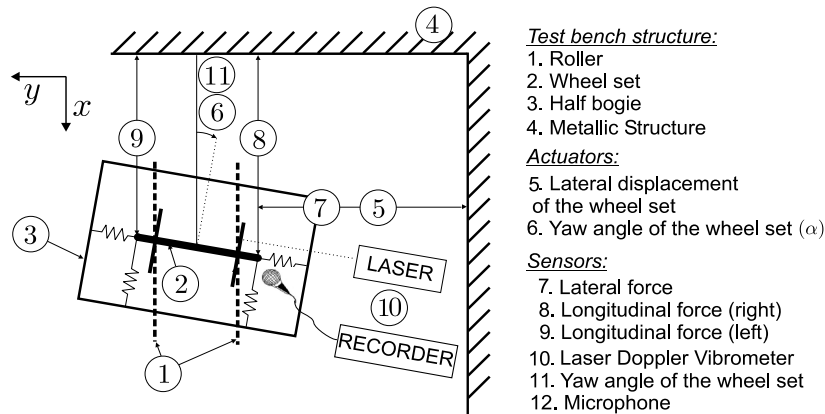where $R_{ij} = R_{ij}^w + R_{ij}^r$ $(i, j = y, z)$.

Fig. 4. Simplified top view of the scaled test bench.

4. Squeal noise model

Squeal models are usually based on the assumption that the surface roughness plays a minor role in the generation of the instability leading to squeal, because in the frequency range of squeal, the wavelength of the irregularity is smaller than the contact patch. If Δz is neglected in Eq. (5), the friction force (Eq. (12)) can be written as a loop gain for the lateral contact force [1]

$$\Delta F_y = \left\{ \frac{\partial F_y}{\partial N} \frac{\Delta N}{\Delta F_y} + \frac{\partial F_y}{\partial \nu_y} \frac{\Delta \nu_y}{\Delta F_y} \right\} \Delta F_y = H(\omega) \Delta F_y \tag{16}$$

where

$$\frac{\Delta N}{\Delta F_y} = \frac{-R_{zy}}{1/k_c + R_{zz}} \text{ and } \frac{\Delta \nu_y}{\Delta F_y} = \frac{i\omega}{V} \left\{ R_{yy} - \frac{R_{yz}^2}{1/k_c + R_{zz}} \right\}.$$

The first term of $H(\omega)$ expresses the coupling between the lateral and the vertical dynamics: the variations of the lateral force are sustained by the variations of the vertical force, leading to a forced vibration of the wheel. The second term of $H(\omega)$ is related to the slope of the friction curve: the higher the decrease after saturation, the higher the self sustained vibrations of the wheel.

If the roughness of the surface is taken into account, it gives an additional variation of the friction force,

$$\frac{\Delta F_y}{\Delta z} = \left\{ R_{yz} + \left(\frac{1}{k_c} + R_{zz} \right) \left[\frac{V - j\omega \frac{\partial F_y}{\partial \nu_y} R_{yy}}{V \frac{\partial F_y}{\partial N} + j\omega \frac{\partial F_y}{\partial \nu_y} R_{yz}} \right] \right\}^{-1} \tag{17}$$

which imposes an additional forced vibration to the wheel.

5. Scaled test bench

The test bench considered in the experiment is a quarter scale roller rig from the New Technologies Laboratory (INRETS), consisting of a scaled wheel set which is rolling on a roller, representing infinite rails [10]. Figure 4 shows a simplified top view of the bench. The wheel set is attached to a half-bogie through geometrically scaled primary suspensions. The roller is driven by an electric motor through a transmission belt. On this bench, the lateral displacement and the yaw angle of the wheel set can be fixed independently. Longitudinal and lateral contact forces are measured with DC force sensors. The half-bogie load is measured with a force sensor. The rotational speed is measured using a tachometer.
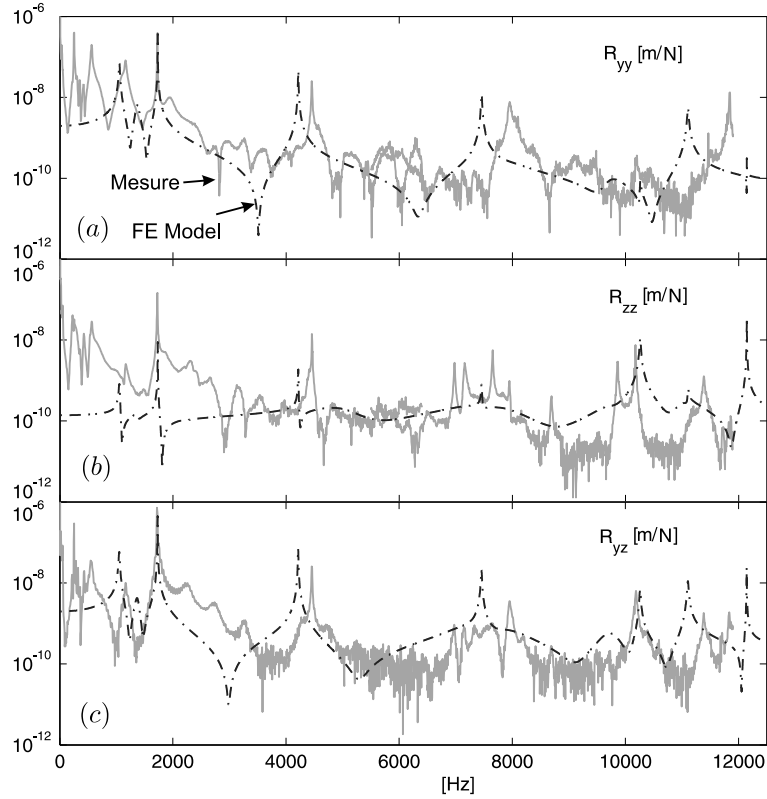
Fig. 5. Dynamics of the wheel: (a) Lateral direct receptance; (b) Vertical direct receptance; (c) Cross receptance between the vertical and the lateral directions.

6. Results

6.1. Squeal noise prediction

The vertical, lateral and cross receptances of the wheel are shown in Fig. 5(a)–(c). For each direction, the receptance measured is compared with those obtained from a finite element model of the wheel.

Figure 6 shows the real part of $H(\omega)$, calculated from the finite element model, and using the following conditions: $N_0 = 3750$ Kg; $C_0 = 8.55$ N$^{1/3}$; $V = 5$ m/s; $\nu_y = 0.01$; $\mu_0 = 0.35$. The highest peak shows the most excited mode, i.e. mode (0L,2) in this case.

6.2. Time histories

First, the friction coefficient between the wheel and the roller has been recorded by imposing a slow variation of the angle of attack from $\alpha = 0$ mrad to $\alpha = 10$ mrad and shown in Fig. 7. The curve is close to the curve measured in dry conditions in [13]. After the saturation, no decreasing slope of the friction curve is visible, neither in [13], nor in this work.

The experiment to reproduce the squeal noise on the scaled bench has been performed in the following conditions:

– Wheel set linear constant speed: $V = 5$ m/s
– Variation of the angle of attack from 0 to 10 mrad (Duration: 15 s)

Figure 8(a) shows the time history of the angle of attack α measured using a contact sensor; Fig. 8(b) shows the lateral speed of the wheel v_y, measured using a laser doppler vibrometer.
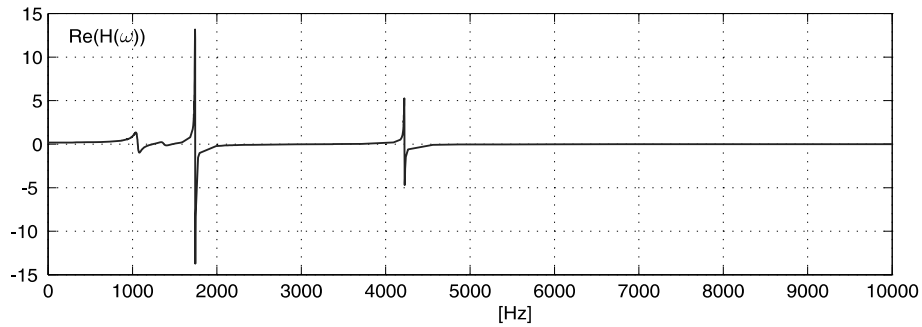
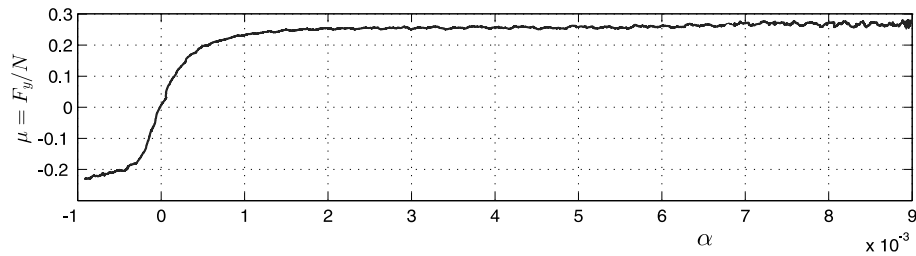Fig. 6. Real part of the transmissibility $H(\omega)$.

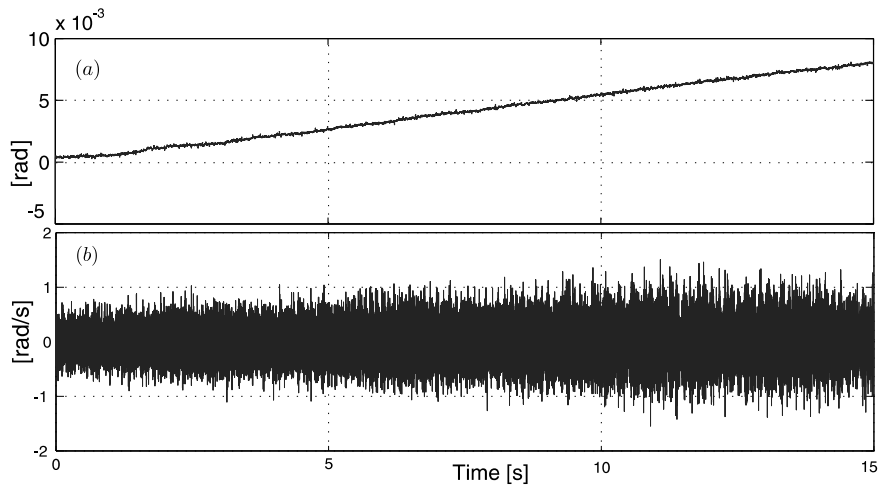Fig. 7. Friction coefficient $\mu = F_y/N$ as a function of the attack angle.

Fig. 8. (a) Angle of attack; (b) Lateral speed of the wheel above the contact point.

Figure 9 shows the frequency spectrum averaged during the time of the experiment of (a) the sound emitted from the wheel-rail contact; (b) the lateral velocity of the wheel set. At high frequency, it shows clearly that the wheel mode (0L,2) is the most excited.

Figure 10 shows the history of the RMS value of (a) the sound emitted from the wheel-rail contact and (b) the lateral velocity of the wheel set during the time of the simulation (i.e. the increase of the attack angle). In order to distinguish between low and high frequency contributions, each figure show also the RMS value of the signal below and above 800 Hz. For both the velocity and the noise, the increase of the RMS value is mainly associated to the high frequency contents of the signal, while the low frequency contribution remains constant.
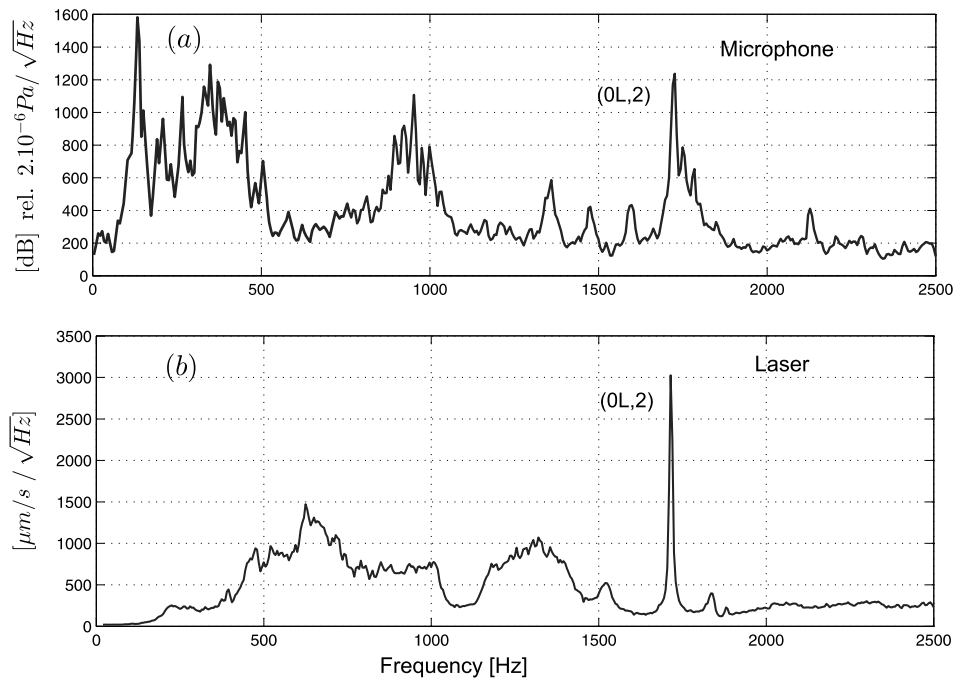
Fig. 9. Frequency spectrum averaged during the time of the experiment of (a) The sound emitted from the wheel-rail contact; (b) The lateral velocity of the wheel set.
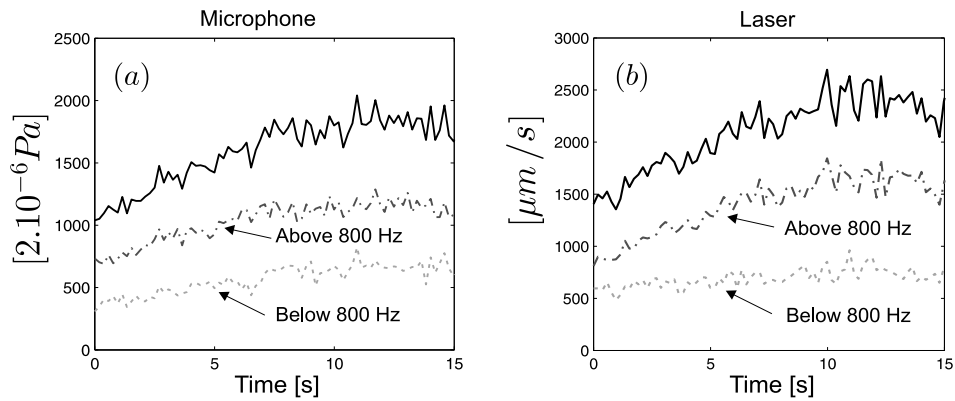

Fig. 10. Time evolution of the RMS value of (a) The sound emitted from the wheel-rail contact; (b) The lateral velocity of the wheel set.

7. Conclusions

The influence of the wheel vertical dynamics in the mechanism of squeal noise has been studied in this work. It has been shown on a single d.o.f. model that the same limit cycle can be generated either by a decreasing slope of the friction curve, or by a vertical excitation of the mass. Then, frequency domain predictions of the instability have been derived, showing two major contributions to the squeal mechanism: self excited and forced vibrations.

An experiment reproducing the squeal noise has been performed on a quarter scaled bench (INRETS). Squeal noise has been correlated to the excitation of mode 0L,2 of the wheel. In this case, as no decrease of the friction curve has been measured, the vertical dynamics of the wheel is found to play a significant role in the wheel squeal mechanism.

Acknowledgments

The author gratefully acknowledge Hugues Chollet and the New Technologies Laboratory of INRETS for supplying the test bench and useful discussions.

References

[1] F.G. de Beer, M.H.A. Janssens and P.P. Kooijman, Squeal noise of rail-bound vehicles influenced by lateral contact position. *Journal of Sound and Vibration* **267** (2003), 497–507.

[2] J.F. Brunel, P. Dufrénoy and F. Demilly, Modelling of squeal noise attenuation of ring damped wheels. *Journal of sound and vibration* **293** (2004), 975–985.

[3] J.F. Brunel, P. Dufrénoy, M. Naît, J.L. a, Munõz and F. Demilly, Transient models for curve squeal noise. *Journal of sound and vibration* **293** (2006), 758–765.

[4] O. Chiello, J.-B. Ayasse, N. Vincent and J.-R. Koch, Curve squeal of urban rolling stock – part 3: Theoretical model. *Journal of sound and vibration* **293** (2006), 710–727.

[5] D.T. Eadie, J. Kalousek and K.C. Chiddick, The role of high positive friction (HPF) modifier in the control of short pitch corrugations and related phenomena, *Wear* **253** (2002), 185–192.

[6] M.A. Heckl and I.D. Abrahams, Curve squeal of train wheels, part 1: Mathematical model for its generation, *Journal of Sound and Vibration* **229** (2000), 669–693.

[7] M.A. Heckl, Curve squeal of train wheels, part 2: Which wheel modes are prone to squeal? *Journal of Sound and Vibration* **229** (2000), 695–707.

[8] M.A. Heckl. Curve squeal of train wheels, part 3: Active control. *Journal of Sound and Vibration* **229** (2000), 709–735.

[9] M. Hinrichs, M. Oestreich and K. Popp, On the modelling of friction oscillators, *Journal of Sound and Vibration* **216** (1998), 435–459.

[10] A. Jaschinski, H. Chollet, S. Iwicki, A. Wickens and J. Von Wurzen, The application of roller rigs to railway vehicle dynamics, *Vehicle System Dynamics* **31** (1999), 345–392.

[11] J.J. Kalker, Survey of wheel-rail contact theory, *Vehicle System Dynamics* **5** (1979), 317–358.

[12] J.J. Kalker and F. Piérard, Wheel-rail noise: Impact, random, corrugation and tonal noise, *Wear* **191** (1996), 184–187.

[13] J.-R. Koch, N. Vincent, H. Chollet and O. Chiello, Curve squeal of urban rolling stock – part 2: Parametric study on a 1/4 scale test rig. *Journal of sound and vibration* **293** (2006), 701–709.

[14] G.L. Kurzweil, Wheel/rail noise-means for control. *Journal of Sound and Vibration* **87** (1982), 197–220.

[15] J. Mandula, B. Salaiova and M. Koval'akova, Prediction of noise from trams, *Applied acoustics* **63** (2002), 373–389.

[16] B. Muller and J. Oertli, Combating curve squeal: Monitoring existing applications. *Journal of sound and vibration* **293** (2006), 728–734.

[17] P. Remignton and J. Webb, Wheel/rail noise reduction through profile modification. *Journal of Sound and vibration* **193** (1996), 335–348.

[18] M.J. Rud, Wheel-rail noise, part I-IV. *Journal of Sound and Vibration* **46** (1976), 359–451.

[19] E. Schneider and K. Popp, Noise generation in railway wheels due to rail-wheel contact forces. *Journal of Sound and Vibration* **120** (1988), 227–244.

[20] G. Sheng, *Friction-induced vibrations and sound: Principles and Application*, CRC Press, 2008.

[21] C. Talotte, P. Van der Stap, M. Ringheim, M. Dittrich, X. Zhang and D. Stiebel, Railway source models for integration in the new european noise prediction method proposed in harmonoise, *Journal of sound and vibration* **293** (2006), 975–985.

[22] N. Vincent, J.-R. Koch, H. Chollet and J.Y. Guerder, Curve squeal of urban rolling stock – part 1: State of the art and field measurements, *Journal of sound and vibration* **293** (2006), 691–700.

[23] U. Wagner, D. Hochlenertb and P. Hagedorn, Minimal models for disk brake squeal, *Journal of Sound and Vibration* **302** (2007), 527–539.